

## CHARACTERIZING GAINP/GAINAS/GE MULTIJUNCTION SOLAR CELLS WITH ELECTROLUMINESCENCE

Thomas Kirchartz<sup>a\*</sup>, Anke Helbig<sup>b</sup>, Martin Hermle<sup>c</sup>, Uwe Rau<sup>a</sup> and Andreas W. Bett<sup>c</sup>

<sup>a</sup>IEF-5 Photovoltaik, Forschungszentrum Jülich, 52425 Jülich, Germany

<sup>b</sup>Institut für Physikalische Elektronik, Pfaffenwaldring 47, 70569 Stuttgart, Germany

<sup>c</sup>Fraunhofer Institut für Solare Energiesysteme, Heidenhofstr. 2, 79110 Freiburg, Germany

\*t.kirchartz@fz-juelich.de

**ABSTRACT:** We show how characterization of GaInP/GaInAs/Ge multijunction solar cells benefits from the use of electroluminescence (EL) measurements. Usual characterization methods involving optical excitation and measurement of electrical response are challenging when they are applied to multijunction concentrator cells due to the necessity of high optical power and the precise simulation of sunlight. By inverting the direction of excitation and response, individual information about the subcells becomes accessible at high injection conditions. We show how to use an electro-optical reciprocity theorem that describes the link between solar cell quantum efficiency and electroluminescent emission to extract the current/voltage curves of the individual subcells from EL spectra. This is accomplished by comparing the spectra with the solar cell quantum efficiency and an independently measured current/voltage curve. The comparison with the solar cell quantum efficiency allows us to determine the relative voltage differences between the three junctions, while the current/voltage curve allows us to adjust the offset of the voltage axis. The final results are internal voltages at all currents, where the spectra were measured. This information yields for example the individual diode quality factors of the cells as well as the difference to their respective radiative limits.

**Keywords:** Multijunction Solar Cells, Electroluminescence, current voltage curves

### 1 INTRODUCTION

The probably most important solar cell characterization technique is the current/voltage curve, which provides basic information about the device: its efficiency, open circuit voltage, short circuit current and fill factor. In many cases, it is desirable to access not only the external voltage at a given current but the actual internal voltage at the collecting junction of the solar cell. This internal voltage is equivalent to the splitting of the quasi-Fermi levels at the junction and is unaffected by the voltage drop over the series resistance. Thus, the internal voltages are on the one hand useful to determine series resistances by comparison with the external voltages and on the other hand they provide information about the recombination dynamic usually expressed by the diode ideality factor  $n_{id}$ . There are two ways to detect this internal voltage. The first possibility is to measure voltages only in open circuit, where the zero current flow over the series resistance leads to the situation that internal and external voltage are the same. This method is termed as either  $\text{suns}/V_{oc}$  or  $J_{sc}/V_{oc}$  [1,2] measurement, since the variation of the current must be realized by a variation of the illumination level. The second possibility is to measure a physical quantity proportional to the internal voltage. Since Würfel's work on the chemical potential of radiation [3], we know that the luminescence emitted by a sample scales proportional to the chemical potential of the photons being in turn proportional to the quasi-Fermi level splitting. The absolute amount of radiation is thus a second possibility to detect internal voltages of a sample [4,5].

Detecting voltages via luminescence has an important advantage when it comes to either modules or multijunction cells. In both cases it is not easily possible to electrically contact individual subcells. Usually only the current/voltage curve of the whole ensemble of several series connected cells is accessible. If for instance one of the series connected cells underperforms, it is possible to distinguish this cell by detecting the internal

current/voltage curve of each cell via electroluminescence.

This article introduces a method to derive the individual current/voltage curves of all subcells in a stacked multijunction cell by combining electroluminescence (EL) and quantum efficiency measurements. The multijunction solar cells under investigation are based on III-V semiconductors on Ge substrate, which have the highest efficiency among today's solar cell technologies [6]. The possibility to grow high quality semiconductor layers epitaxially on top of each other allows a better adaptation of the absorber materials to the solar spectrum [7]. Using luminescence techniques in III-V based semiconductors is very appropriate since these materials have a high radiative recombination rate and are therefore highly luminescent. These high efficiency multijunction cells are often used in concentrator applications, where the device performance under higher injection conditions is

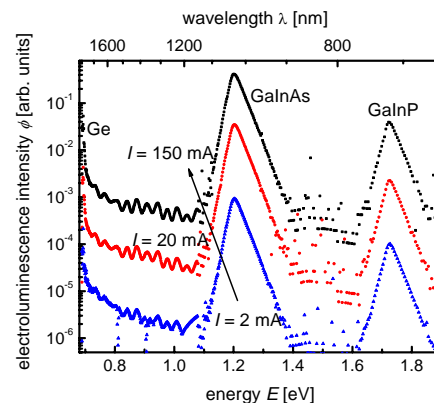


**Figure 1:** Electroluminescence (EL) spectra of the multijunction cell at three different injection currents ( $I = 2, 20$ , and  $150$  mA).

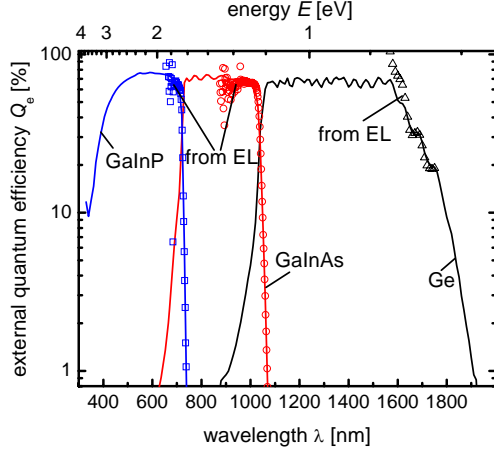


**Figure 2:** Comparison of the directly measured quantum efficiency (solid lines) to the quantum efficiencies derived from the EL spectrum (symbols) using Eq. (1).

of interest. For luminescence measurements, higher injection conditions are relatively easy to realize since the luminescence increases with injection current, making the signal detection easier with higher injection conditions.

## 2 EXPERIMENTAL

We measure the EL spectra of a lattice mismatched  $\text{Ga}_{0.35}\text{In}_{0.65}\text{P}/\text{Ga}_{0.83}\text{In}_{0.17}\text{As}/\text{Ge}$  solar cell at currents ranging from 100  $\mu\text{A}$  to 150 mA and over a range of wavelengths  $\lambda$  from 600 nm to 1800 nm. The solar cell of an area  $A = 0.032 \text{ cm}^2$  was prepared by metal organic vapor phase epitaxy [8]. The current is applied with a DC current source and the EL emission is chopped in order to allow the use of lock-in amplifiers. The spectra are then recorded with a Ge detector attached to a single stage monochromator and are subsequently corrected for the relative sensitivity of the setup.

## 3 THEORY

The basic theoretical ingredient for our analysis is the spectral reciprocity relation (RR) between solar cell and light emitting diode (LED) as described in Ref. [9] and experimentally verified for the case of pn-junction solar cells made of Si and  $\text{Cu}(\text{In,Ga})\text{Se}_2$  [10,11]. The RR relates the external solar cell quantum efficiency  $Q_e(E)$  to the spectral emission  $\phi_{\text{em}}$  via [9]

$$\phi_{\text{em}}(E) = Q_e(E) \phi_{\text{bb}}(E) \left[ \exp\left(\frac{qV}{kT}\right) - 1 \right], \quad (1)$$

where  $\phi_{\text{bb}}(E)$  is the black body photon flux,  $V$  is the internal voltage applied to the pn-junction, and  $kT/q$  is the thermal voltage. Equation (1) connects the spectral EL emission with two quantities of high relevance for photovoltaics: with the quantum efficiency  $Q_e(E)$  and the junction voltage  $V$ . In the following, we determine the three junction voltages  $V_j$  ( $j = 1, 2, 3$ ) of the three individual subcells of our  $\text{GaInP}/\text{GaInAs}/\text{Ge}$  stack.

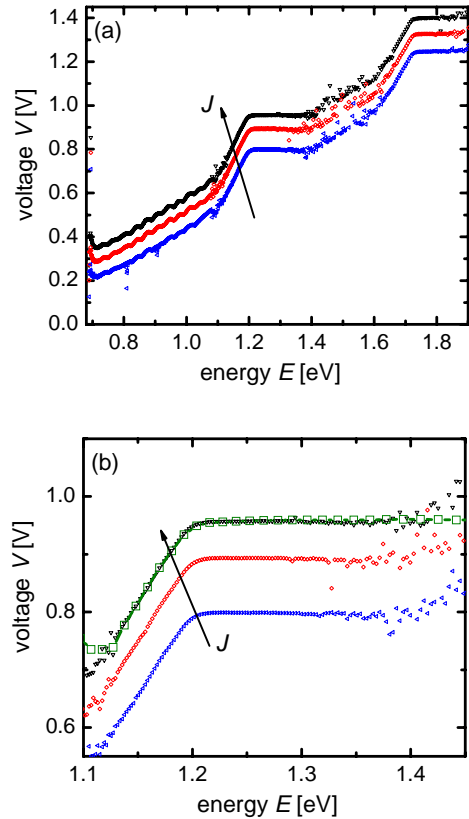
Therefore, we use directly measured external quantum efficiencies  $Q_e^{\text{dir}}$  to scale EL emission of each subcell with the help of Eq. (1).

## 4 RESULTS

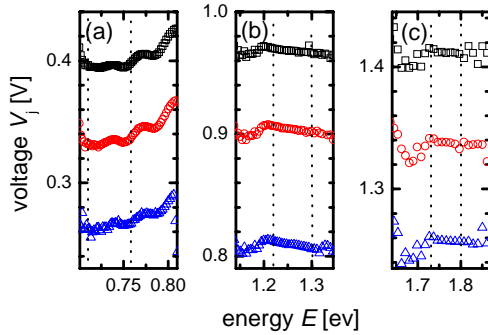
### 4.1 Electroluminescence and quantum efficiency

Figure 1 shows three exemplary EL measurements at currents  $I = 2, 20$ , and 150 mA. The spectra feature two pronounced peaks of the direct semiconductors  $\text{GaInAs}$  ( $E \approx 1.20 \text{ eV}$ ) and  $\text{GaInP}$  ( $E \approx 1.72 \text{ eV}$ ). The Ge peak is hardly visible since the sensitivity of the Ge detector is already very low at the peak around  $E \approx 0.70 \text{ eV}$ .

Figure 2 shows  $Q_e^{\text{dir}}$  of the three subcells measured directly (using the method described in Ref. [12]) in comparison to the quantum efficiency  $Q_e^{\text{EL}}$  extracted from the EL spectrum taken using Eq. (1). For the  $\text{GaInAs}$  and  $\text{GaInP}$  solar cells, we find a good agreement of the respective low-energy portions of  $Q_e^{\text{dir}}$  and  $Q_e^{\text{EL}}$  including a part of the region where the quantum efficiency saturates. At higher photon energies,  $Q_e^{\text{EL}}$  becomes noisy because of the low intensity of the underlying EL signal (Fig. 1). For the Ge cell, the spectral region, where  $Q_e^{\text{dir}}$  and  $Q_e^{\text{EL}}$  correspond to each other is restricted to the high wavelength slope, whereas



**Figure 3:** (a) Internal voltage derived from the EL spectra of Fig. 1 according to Eq. (3) showing three steps for the three absorbers. the measurements are presented for the same three currents as in Fig. 1 (b) Detail of (a) with a focus on the middle cell ( $\text{GaInAs}$ ). The directly measured quantum efficiency is shown for comparison (dashed line with open squares).



**Figure 4:** (a, b, c) Relative internal voltage derived from the EL spectra of Fig. 1 according to Eq. (3) for currents  $I = 2$  mA (open triangles), 20 mA (circles), 150 mA (squares). The dotted vertical lines indicate the spectral intervals, where the voltages have been determined.

at higher photon energies ( $> 0.76$  eV) and lower wavelengths ( $< 1630$  nm) the original EL is distorted by stray light. Due to the exponential energy dependence of the black body spectrum in Eq. (1), the increased luminescence signal strongly affects the  $Q_e^{\text{EL}}$  leading to the discrepancy to  $Q_e^{\text{dir}}$ , visible in Fig. 2.

#### 4.2 Determination of internal junction voltages

In order to determine the internal junction voltages, we have to consider the fact that the EL intensity is measured in arbitrary units, and thus reformulate Eq. (1) using the Boltzmann approximation for  $\phi_{\text{bb}}$  as

$$\phi_{\text{em}}(E) = C Q_e(E) E^2 \exp\left(\frac{-E}{kT}\right) \exp\left(\frac{qV}{kT}\right), \quad (2)$$

with  $C$  being an unknown energy independent proportionality factor. Solving for the internal voltage  $V_j$  at any of the three junctions  $j = 1, 2, 3$  leads to

$$V_j = V_T \ln(\phi_{\text{em}}) + E/q - 2V_T \ln(E) - V_T \ln(Q_e^j) - V_T \ln(C), \quad (3)$$

with  $V_T = kT/q$ . Except for the constant additive term  $\delta V = V_T \ln(C)$ , Eq. (3) enables us to determine the voltage that internally drops over each of the three pn-junctions.

In order to understand the meaning of Eq. (3), we proceed in two steps. First, we assume that we don't know the directly measured quantum efficiencies from another measurement and interpret  $V_T \ln(Q_e)$  as an unknown. Performing the operation in Eq. (3) on the measured spectra of Fig. 1 then leads to Fig. 3a. The shape of the spectra is now like a staircase with a step for each of the three absorbers. Between the spectral regions of the peaks, there are large areas visible, where the signal is either noise or stray light and therefore not useful for our investigation. For the Ge cell, no step is visible from the EL measurements, which corresponds to the result of Fig. 2. According to Eq. (3), the voltage axis is equivalent to a logarithmic quantum efficiency axis. Hence, we can insert the directly measured quantum

efficiencies (solid lines) from Fig. 2 to show the regions, where the staircase corresponds to the quantum efficiencies. Fig. 3b compares the voltage obtained from Eq. (3) with the direct quantum efficiency of the GaInAs cell from Fig. 2.

Is it now possible to determine the internal voltages, if we do not know the quantum efficiency. This works as long as the quantum efficiencies in the saturation regions are similar. Then we could determine the voltage for a given injection current from the three plateaus in Fig. 3a. The error in voltage would be given by the variation in  $V_T \ln(Q_e)$  between the three cells. However in the present case, this is not advisable since the Ge cell does not form a clear plateau due to the severe stray light problems in the single stage monochromator.

The most secure way to determine the internal voltage as a function of the applied current is therefore to evaluate the EL spectra modified by Eq. (3) at energies, where they correspond to the directly measured quantum efficiency. In this case, we include the term  $V_T \ln(Q_e)$  for each of the three cells individually. Thus we account for both variations in the saturation level of the quantum efficiency as well as stray light.

Figures 4a-c show the result of performing the operation given by Eq. (3) on the measured spectra of Fig. 1. The three spectral regions highlighted by vertical lines in Figs. 4a-c correspond to the ranges, where the EL of each subcell yields a maximum signal and where  $Q_e^{\text{dir},j} \approx Q_e^{\text{EL},j}$  in Fig. 2. Since the internal voltages are the quasi Fermi-level splittings at the three internal junctions, the application of Eq. (3) in these regions must lead to a result for  $V_j$  being independent of energy. This is verified by Figs. 4a-c.

The constant offset voltage  $\delta V$  is determined from a separately measured current/voltage ( $J/V$ ) curve under about 25 suns illumination as depicted in Fig. 5. Then we adjust the sum  $\Sigma V_j$  of the junction voltages (measured at a dark current density  $J_D$ ) to the open circuit voltage  $V_{\text{OC}}$  at the illumination condition leading to the corresponding short circuit current density  $J_{\text{SC}} = J_D$ . Note that this scaling must only be performed once for the total series of EL measurements because the offset voltage  $\delta V$  is the same for all spectra. Adjusting the voltages to  $V_{\text{OC}}$  and not to an arbitrary voltage is

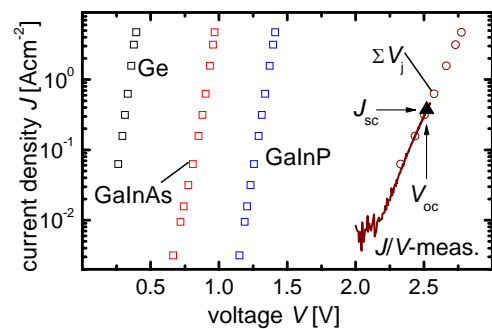


**Figure 5:** The voltages (open circles) obtained from Fig. 4 are adjusted to the open circuit voltage  $V_{\text{OC}}$  (full triangle) of a current/voltage ( $J/V$ )-curve under 25 suns illumination. The solid line represents this  $J/V$  curve shifted by the short circuit current density  $J_{\text{SC}}$ . We finally receive the  $J/V$ -curves of the three individual subcells (open squares) with a correctly scaled voltage axis.

necessary since neither the internal voltages from EL nor the  $V_{OC}$  contain resistive effects as any other directly measured voltages do.

Having determined the offset voltage, we can rescale the voltage axis in Figs. 4a-c and finally receive the internal voltages of the individual subcells, shown in Fig. 5 for a wide range of injection currents. Summing up the individual voltages leads to  $\Sigma V_j$  as a function of injection current. This curve nicely corresponds to the directly measured  $J/V$ -curve over the whole range and not only at the point  $V = V_{OC}$  (which is the case by design).

#### 4.3 Diode quality factors

From the semilogarithmic slope of the  $J/V$ -curves, we determine the diode quality factors  $n_{id}$  with the relation

$$n_{id} = q/kT \times \partial V / \partial \ln J, \quad (4)$$

receiving the values  $n_{id} = 1.14, 1.61$ , and  $1.37$  for the Ge, GaInAs, and GaInP cell, respectively. Thus, the Ge cell has a rather ideal current/voltage curve, with an ideality factor close to one in contrast to the other two subcells. For the two direct semiconductors, the ideality factor is higher, which hints to a non ideal recombination current in this subcells. As a small concentrator cell with a large edge to area ratio was investigated, leakage currents at the cell edge are most likely the reason of this non ideal behavior. For the determination of  $n_{id}$ , we used a linear fit of  $\ln(J)$  for all datapoints and thus, did not distinguish between the ideality at low and high injection. Figure 5 indicates, that all datapoints of the Ge cell are at high injection, whereas the datapoints of the GaInAs and GaInP cell cover the injection range from low to higher injection. As the influence of the edge leakage currents decrease with increasing injection level the determined diode quality factors for the upper subcells comprises the low and high injection diode quality factors, where the diode quality factor of the Ge cell neglected the low injection range.

#### 4.4 Radiative saturation current density

Apart from measuring the internal voltages, we can also rate the quality of the subcells from the difference between these internal voltages and their respective radiative limits. The saturation value  $J_{0,rad}^j$  of the radiative recombination current of cell  $j$  follows directly from Eq. (1) via [10,11]

$$J_{0,rad}^j = q \int Q_e^j(E) \phi_{bb}(E) dE. \quad (5)$$

Defining the radiative open circuit voltage by

$$V_{OC,rad}^j = V_T \ln(J_{SC} / J_{0,rad}^j) \quad (6)$$

allows us to determine  $V_{OC,rad}^j$  for each subcell. The difference

$$\Delta V_{OC} = V_{OC,rad}^j - V_j(J = J_{SC}) \quad (7)$$

is then a measure for non-radiative recombination losses in the subcell [10,11]. The resulting values at the injection current of the  $J/V$ -measurement (25 suns) are  $\Delta V_{OC} = 226$  mV,  $132$  mV, and  $210$  mV for the Ge, GaInAs, and GaInP cell, respectively. Hence, the GaInAs cell comes by far closest to its radiative limit.

## 5 CONCLUSIONS

By combining EL and quantum efficiency measurements, the present method allows us not only to determine the internal voltages of stacked multijunction solar cells but also to evaluate the performance of each subcell with respect to the respective radiative limit.

## ACKNOWLEDGEMENTS

The authors want to thank R. Carius for fruitful discussions and G. Fritsch for help with the calibration of our set-up and R. Hoheisel and A. Wekkeli for the measurement of the EQE and IV-curve.

## REFERENCES

- [1] A.G. Aberle, S.R. Wenham, M.A. Green, in: Proceedings of the 23rd IEEE Photovoltaics Specialists Conference, IEEE, New York, 1993, pp. 133–139.
- [2] P. J. Rostan, U. Rau, V. X. Nguyen, T. Kirchartz, M. B. Schubert, and J. H. Werner, Sol. Ener. Mat. Sol. Cells **90**, 1345 (2006).
- [3] P. Würfel, J. Phys. C: Solid State Phys. **15**, 3967 (1982).
- [4] T. Trupke, R. A. Bardos, M. D. Abbott, and J. E. Cotter, Appl. Phys. Lett. **87**, 093503 (2005).
- [5] T. Kirchartz, U. Rau, M. Hermle, A. W. Bett, A. Helbig, and J. H. Werner, Appl. Phys. Lett. **92**, 123502 (2008).
- [6] M. A. Green, K. Emery, Y. Hisikawa, and W. Warta, Prog. Photovoltaics, **15**, 425 (2007).
- [7] F. Dimroth and S. Kurtz, MRS Bull. **32**, 230 (2007).
- [8] F. Dimroth, phys. stat. solid. (c) **3**, 373 (2006).
- [9] U. Rau, Phys. Rev. B **76**, 085303 (2007).
- [10] T. Kirchartz, U. Rau, M. Kurth, J. Mattheis, and J. H. Werner, Thin Solid Films **515**, 6238 (2007).
- [11] T. Kirchartz and U. Rau, J. Appl. Phys. **102**, 104510 (2007).
- [12] M. Meusel, C. Baur, G. Létay, A. W. Bett, W. Warta, and E. Fernandez, Prog. Photovoltaics **11**, 499 (2003).